ELSEVIER

PII: S1359-835X(97)00079-1

Composites Part A **29A** (1998) 283–291

1359-835X/98/$19.00

Toughness of the fiber/matrix interface in nylon-6/glass fiber composites†

A. Pegoretti[a,*], M. Fidanza[a], C. Migliaresi[a] and A. T. DiBenedetto[b]
[a]*Department of Materials Engineering, University of Trento, via Mesiano 77, 38050 Trento, Italy*
[b]*Department of Chemical Engineering and Institute of Materials Science, University of Connecticut, Storrs, CT 06269-3136, USA*
(Received 4 March 1997; revised 2 July 1997; accepted 4 August 1997)

The aim of the present study is to investigate the effects of the temperature and fiber surface finishing on the interfacial fracture toughness of nylon-6/E-glass fibers composites. The fracture toughness evaluation is based on a new method, recently proposed by the authors, which yields the strain energy release rate associated with the fiber/matrix interfacial debonding, G_{arrest}, as a combination of a finite element analysis and experimental measurements on embedded single fiber microcomposites. For the unsized E-glass fibers an interface toughness of 165 Jm^{-2} has been found, while for the polyamide and epoxy compatible sized E-glass fibers higher interfacial debonding energy values of about 340 Jm^{-2} have been measured. Both sized and unsized E-glass fiber microcomposites showed a strong decrease of the interfacial toughness as the temperature increased.

(Keywords: B. fragmentation; C. finite element analysis (FEA); interface toughness)

INTRODUCTION

It is well-known that the level of adhesion between fibers and matrix plays a major role in determining the mechanical performances and environmental stability of most types of advanced composite materials. Among the many obstacles to progress in this area has been a lack of adequate experimental techniques for quantitatively determining bond mechanical properties.

A great deal of past work dealing with fiber/matrix interfacial strength measurements has focused on the development of reliable experimental test procedures[1,2]. The most common methods involve the use of single fiber composites in order to perform micromechanical tests, such as the fragmentation test[3,4] and a variety of single fiber pull-out[5], microdebond[6] and microindentation tests[7]. One of the most widely studied is the 'embedded single fiber' or fragmentation test in which a single fiber is embedded in the centerline of a matrix tensile specimen. Upon application of a tensile force the embedded fiber breaks repeatedly at points where the fiber strength has been reached. Continued application of strain to the specimen results in fiber fragments so short that the shear stress transfer along their lengths can no longer build up enough tensile stress to cause further failures, and a limiting fragment size, defining a critical length l_c, is reached ('saturation'). From the value of l_c and the extrapolated fiber mean strength at the critical length, a mechanical parameter called 'interfacial shear strength' (ISS) is usually obtained on the basis of a simplistic force equilibrium, based on shear-lag or elastic–plastic stress analyses. A more rigorous treatment of the experimental data necessarily requires to deal with the complexity of the interfacial stress state[8,9] and with a very careful handling of the Weibull statistics in order to avoid errors due to the extrapolation of the fiber strength to very small lengths[10,11]. Moreover, in many experimental situations, the lack of a saturation state (brittle matrices) and/or the presence of relevant interfacial debonding, friction, and plastic yield, further contribute to the inapplicability of the classical stress-based theories.

Consequently, in order to overcome some of these difficulties and limitations, recently some authors proposed various energy-based approaches to the fragmentation test with the aim to evaluate the mechanical energy required to decouple a fiber from the matrix rather than the maximum stress transferability. Reviewing the results of the embedded single fiber test in E-glass and carbon fiber reinforced polymer microcomposites, DiBenedetto[12] proposed a fracture energy criterion based on a finite element analysis of the fiber-matrix decoupling process. In particular, E-glass fiber systems appeared to be bounded by fracture energies of the order of 230 Jm^{-2} for well-bonded interfaces to 60 Jm^{-2} for poorly-bonded interfaces, with values being

* To whom correspondence should be addressed
† Dedicated to the memory of Professor P. G. Orsini

slightly influenced by temperature. Further developments of the finite-element analysis allowed DiAnselmo *et al.*[13] to evaluate the effect of interphase stiffness and strength on fracture toughness by calculating the energy release rate, G, associated with interface debonding at a specified level of strain. A finite element analysis of a single fiber embedded in a polymer matrix was used by DiBenedetto *et al.*[14], and Jones and DiBenedetto[15] to simulate the effects of interphase toughness and stiffness on the mode of crack propagation from a broken fiber end. The failure process arising at a broken fiber end in polymer matrix composite materials has been recently studied, experimentally and analytically, by the authors[16] using a finite element method. A series of experiments was carried out using S-glass and E-glass single filaments, with various sizings and/or coupling agents, embedded in epoxy matrices with different moduli. Cracks have been observed to propagate from the broken fiber end either by interfacial debonding, shear conical matrix cracks, transverse matrix cracking, or a combination of the three modes. A dynamic strain energy release rate upon arrest of an interfacial crack, G_{arrest}, varying from 57 to 342 Jm^{-2}, was measured, depending primarily on the nature of the fiber sizing and the ratio of moduli of the fiber and matrix.

An energy-based interpretation of the fragmentation experiments has been also proposed by Wagner and co-workers [17,18] in order to analyse the experimental results of composite systems that never reach saturation, like E-glass fibers/epoxy aged in hot distilled water. Further refinement of the energy balance allowed Wagner *et al.* [19] to present a one-dimensional theoretical model for the energy necessary to initiate/nucleate an interfacial crack from its associated transverse fiber break during a single fiber fragmentation test. In the case of unsized and sized E-glass fibers embedded in an UV-cured polymeric matrix, they reported interface energies of 183 Jm^{-2} and 264 Jm^{-2}, respectively. An in-depth examination of the relative roles of the physical parameters that appear in such a theoretical model is reported in ref.[20].

Recently, Copponex[21] improved the Nairn's[22] variational mechanics approach to the single fiber fragmentation test, taking into account imperfect adhesion and finally derived an interfacial debonding criterion by means of an energy release rate analysis. Experimental tests performed on different E-glass/polypropylene microcomposites led to G_{IIC} values of the order of 45 Jm^{-2} for the pure polypropylene matrix and 183 Jm^{-2} for modified polypropylene matrix.

The great interest towards the development of an energy-based fracture mechanics approach to the fiber/matrix decoupling phenomenon is furthermore documented by the number of new models recently proposed to interpret the single fiber pull-out and microdebonding tests[23–29].

The aim of this paper is to study the fracture toughness of the fiber/matrix interface in E-glass/nylon-6 model composites by an energy-based approach of the fragmentation test. The method, recently proposed by the authors[16], involves the experimental determination of the fiber/matrix fracture parameters and the finite element analysis of the debonding process. In the present work, the effects of fiber radius, fiber surface finishing and test temperature on the strain energy release rate associated with the propagation of an interfacial crack were evaluated.

EXPERIMENTAL

Materials

The matrix of the microcomposites used in this work was a nylon-6 film (SNIA S.p.A., Italy) extruded with a thickness of about 50 μm. After drying under vacuum at a temperature of 100°C for 48 h, the films were stored under vacuum in a desiccator until use.

The following E-glass fibers were used as-received:

(1) Sisecam, (Sisecam, Turkey), nominal diameter 14 μm, both unsized and surface treated with a commercial polyamide compatible coupling agent;
(2) PPG 2001 (PPG, The Netherlands) nominal diameter 24 μm, surface treated with a commercial epoxy compatible coupling agent.

The microcomposite samples were prepared according to the following procedure: (i) two flat aluminum plates were surface mirror-polished and covered with a mold releasing agent; (ii) about 15 fibers were carefully aligned within two nylon-6 films sandwiched between the aluminum plates; (iii) the mold was placed in an oven under vacuum at a temperature of 300°C and at a pressure of about 10 kPa for 50 min; (iv) after cooling in air, samples were obtained by cutting strips (4 × 45 × 0.090 mm^3) containing one single fiber each, longitudinally aligned in the centerline. Before testing, all the samples were exposed at the laboratory conditions till a constant weight was reached.

Matrix properties

Differential Scanning Calorimetry (DSC) measurements were performed by a Mettler DSC 30 apparatus, at a heating rate of 10°C min^{-1}, under a nitrogen flux of 10 ml min^{-1}. The dry films showed a glass transition temperature of 42°C, a melting temperature of 222°C and a crystallinity content equal to 28.6% by weight.

Tensile tests were performed on strip samples (4 × 75 × 0.090 mm^3) with a gage length of 40 mm by using an Instron 4502 tensile tester equipped with a thermostatic chamber (model 3119) at strain rate of 0.008 min^{-1}.

Dynamic-mechanical tests were conducted in the tensile mode by a dynamic mechanical thermal analyser (DMTA, model MKII, by Polymer Laboratories), at a frequency of 1 Hz and a heating rate of 3°C min^{-1}.

Fibers properties

The fiber diameters were measured using an optical microscope (Ortholux II POL-BK by Leitz) and an image analyser system (MET1 by Pertel) at a magnification of 200 ×. Tensile strength and strain at break were measured

Table 1 Strain at break, and Weibull strength parameters of the E-glass fibers used in the present work

Fiber	Sizing	Strain at break (gage length = 25 mm) ϵ_b (%) {No. of specimens}	Weibull scale parameter (referred to a gage length = 5 mm) α (MPa) {No. of specimens}	Weibull shape parameter β
Sisecam	none	2.53 ± 0.88 {47}	1995 {158}	4.010
Sisecam	polyamide compatible	3.76 ± 0.66 {66}	2798 {167}	6.255
PPG 2001	epoxy compatible	3.79 ± 0.97 {50}	3020 {133}	3.934

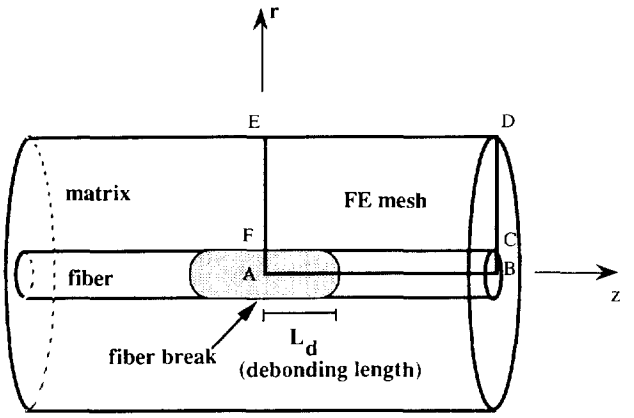

Figure 1 Schematic drawing of the fiber break and associated interfacial debonding length (L_d). The region ABDE was considered for the FE analysis

at various gage lengths on monofilaments randomly extracted from a bundle of the fiber to be tested. According to the ASTM standard D3379-75, a single fiber was centerline mounted on window cards using a quick-setting glue and tested at room temperature and a cross-head speed of 0.2 mm min^{-1} using an Instron machine equipped with a 10 N load cell.

Weibull shape, α, and scale, β, parameters (reported in *Table 1*) were determined from strengths measurements performed at various gage lengths following an iterative procedure recently proposed by Gurvich *et al.*[30] Sisecam fibers (both treated and untreated) were tested at gage lengths of 25, 20, 15, 10 and 5 mm, while PPG fibers were tested at gage lengths of 40, 25, 20, 10 and 5 mm. The average strength $\bar{\sigma}_{fb}(L)$ at an arbitrary length L may then be calculated as:

$$\bar{\sigma}_{fb}(L) = \alpha\left(\frac{L}{L_0}\right)^{-1/\beta}\Gamma(1+1/\beta) \qquad (1)$$

where L_0 is the reference length and Γ is the gamma function.

Embedded single fiber test

Fragmentation experiments were performed at two different temperatures (20 and 100°C) by using a custom-made apparatus[31] consisting of a small tensile tester (Minimat, by Polymer Laboratories), equipped with a thermostatic chamber, and put under a polarized optical stereo-microscope (Wild M3Z by Leica). This apparatus allowed us to apply a constant strain rate (fixed at 0.008 min^{-1}) and to record the stress–strain behavior of the sample. At least five samples were tested for each experimental condition. At the first fiber break the test was stopped and the sample unloaded in order to correctly measure the interfacial debonding. Due to the relatively low fiber strain at break ($< 4.5\%$), no slippage was supposed to occur between fiber and matrix and the fiber strain was considered equal to the sample strain. Soon after the sample was reloaded till a strain of 20% in order to assure the saturation of the fragmentation process and the mean fiber length, $\bar{L}_s$, was measured. As proposed by Ohsawa *et al.*[32], the fiber critical length, L_c, was considered equal to $(4/3)\bar{L}_s$. The interfacial shear strength (ISS) was evaluated following the simplified physical model proposed by Kelly and Tyson [3], which yields the well-known expression:

$$\mathrm{ISS} = \frac{\bar{\sigma}_{fb}(L_c)d}{2L_c} \qquad (2)$$

where $\bar{\sigma}_{fb}(L_c)$ is the mean fiber strength at the critical length.

Finite element (FE) analysis

In order to evaluate the total stored elastic energy, U, and the strain energy release rate, G, a stress FE analysis was performed for each fiber-matrix combination. As reported in ref.[16] the microcomposite specimen was modeled as a cylinder of matrix surrounding a single fiber (*Figure 1*). The FE mesh covered one quadrant of the cylinder with AB and AE as axes of symmetry. AF was taken equal to the nominal fiber radius r_f (see Experimental), the outer radius of the cylinder (AE) was fixed equal to 45 μm, and the half-length of the fiber AB was taken equal to 125 μm (i.e. 2.5 times the maximum crack length). It is worth noting that the diameter of the modeled cylinder is equal to the actual thickness of the microcomposites used for experimental measurements. The following boundary conditions were applied to the model:

(1) side AB, zero displacement in the r direction (from symmetry condition);
(2) side BCD, uniform displacement in the z direction (from experimental condition);
(3) side DE, free surface (from experimental condition);
(4) side EF zero displacement in the z direction (from symmetry condition).

Linear elastic behavior was assumed (the mechanical properties used in the FE model are reported in *Table 2*) with no slippage between fiber and matrix along the bounded interface, and no friction on the debonded fiber length.

A commercial package PATRAN® 2.5 was used to

generate a FE mesh consisting of four-node quadrilateral axisymmetric elements with an aspect-ratio varying from 1 (near the debonding zone) to 3 (far from the crack). 8050 and 9240 elements were used for the Sisecam and PPG 2001 fiber systems, respectively. The solution was obtained using a commercial FE code ABAQUS® 5.5-2.

To simulate the crack propagation, an automated procedure was assessed in order to progressively release the duplicated interfacial nodes along the line FC. In this way, the propagation of an interfacial crack, L_d, from 0 to 50 μm, was simulated at steps of 0.5 μm initially (for a length equal to one fiber radius) and 1 μm afterwards. For each crack length, the total stored elastic energy, U, of the system was computed as follows:

$$U = \frac{1}{2}\int \sigma \epsilon dV \approx \frac{1}{2}\sum_i F_i \delta_i = \delta \frac{1}{2}\sum_i F_i \qquad (3)$$

where F_i and δ_i are the forces and displacements, respectively, on the nodes along the line BD of the model, and V is the volume of the model.

Table 2 Material properties used for the FE analysis

Material	Temperature (°C)	Tensile modulus E (GPa)	Poisson's ratio ν
E-glass	20 ÷ 100	70[a]	0.22[a]
Nylon 6	20	2.0[b]	0.33[c]
	100	0.5[c]	0.46[c]

[a] From ref. [33]
[b] From DMTA measurements
[c] From ref. [34]

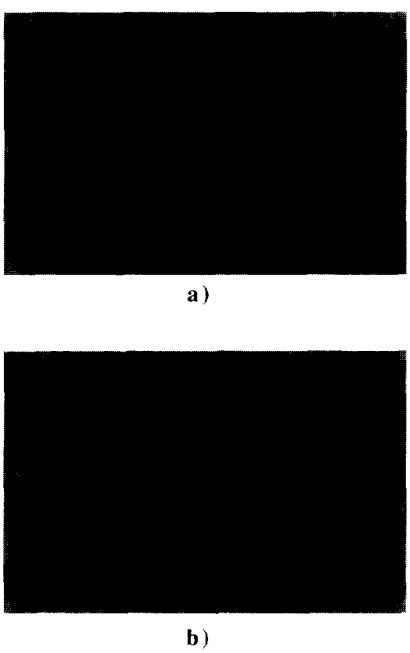

Figure 2 Optical photomicrographs (200 ×) of the first break of a single PPG 2001 E-glass fiber embedded in a nylon-6 matrix and tested at (a) 20°C and (b) 100°C, respectively

RESULTS AND DISCUSSION

When a continuous filament embedded in a polymer matrix is broken under tension, the released energy is usually enough to generate fractures in the matrix and/or along the interphase. Three modes of failure are commonly observed, i.e. a penny-shaped matrix crack perpendicular to the fiber axis, two inclined conical matrix cracks emanating from both broken fiber ends, and an interfacial debonding running parallel to the fiber surface[35,36]. Combinations of these fracture patterns have also been observed[16].

In the present study, regardless of the fiber surface treatment and the test temperature, we always observed interfacial debonding characterized by a crack running parallel to the fiber surface along the interface as reported in *Figure 2* for the nylon-6 microcomposites reinforced with PPG 2001 E-glass fibers.

The experimentally observed strain at the first fiber break and the corresponding debonding length (L_d in *Figure 1*), for various fibers at 20°C and 100°C, are reported in *Table 3*. The strain at the first fiber break measured on the microcomposites was similar to the fiber strain at break tested in air, for fibers of 25 mm gauge length (*Table 1*). As the test temperature increased, the values of strain at first fiber break were found to slightly decrease. This behavior can be attributed to relaxation of the thermal compressive residual stresses developed in the fiber during the cooling of the microcomposites after molding, as already observed in nylon-6/carbon fiber microcomposites[37]. From *Table 3* it can be observed that, for all the systems under investigation, the temperature increase resulted in higher values of the debonding length. In particular, at a test temperature of 100°C, the elastic strain energy released after the first fiber fracture led to interfacial debonding lengths 1.5–2.3 times higher than those obtained at room temperature. Moreover, from *Table 3* it can be observed that an increase of the test temperature caused an increase in the fiber critical aspect ratios. The temperature dependence of the

Table 3 Strain and corresponding debonding length at first fiber break, and critical aspect ratio at saturation, evaluated at different temperatures for various nylon-6/E-glass fiber microcomposites

Fiber	Sizing	Test temperature (°C)	Strain at first fiber break (%)	Debonding length at first fiber break L_d (μm)	Critical aspect ratio at saturation L_d/d
Sisecam	none	20	2.65 ± 0.10	5.2 ± 1.0	57.5 ± 4.5
		100	2.43 ± 0.12	8.0 ± 0.7	74.9 ± 7.6
Sisecam	polyamide compatible	20	4.18 ± 0.52	7.4 ± 1.3	53.6 ± 4.0
		100	3.98 ± 0.31	11.5 ± 2.1	85.7 ± 11.0
PPG 2001	epoxy compatible	20	3.70 ± 0.15	11.3 ± 1.2	73.5 ± 6.1
		100	3.58 ± 0.29	19.5 ± 1.8	106.6 ± 27.7

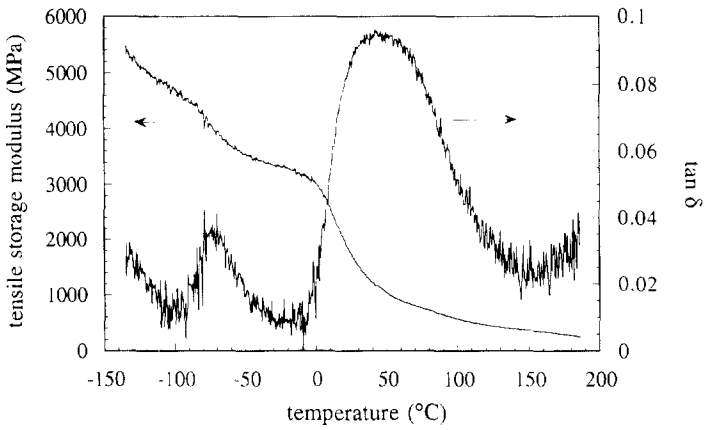

Figure 3 Matrix tensile storage modulus and loss factor versus temperature

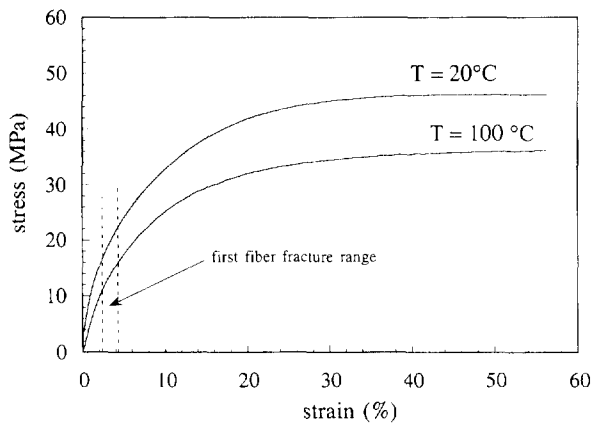

Figure 4 Effect of temperature on the matrix stress–strain curve

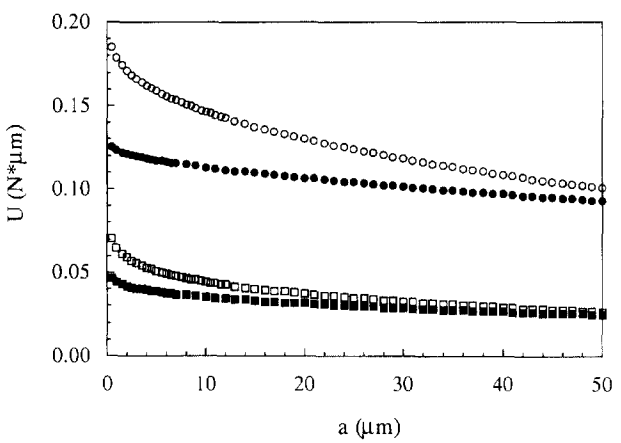

Figure 5 Elastic strain energy, U, as a function of the crack length, a, evaluated by the FE analysis for nylon-6 matrix composites reinforced with various E-glass fibers at different temperatures. Analyses refer to a strain of 1%. (●) Sisecam, diameter 14 μm, temperature 20°C; (■) Sisecam, diameter 14 μm, temperature 100°C; (○) PPG 2001, diameter 24 μm, temperature 20°C; (□) PPG 2001, diameter 24 μm, temperature 100°C

critical fiber length in polymer matrix composites was firstly studied by Ohsawa *et al.*[32] using the single fiber fragmentation test. For glass fiber-reinforced polyester resin they found that the critical aspect ratio greatly increased with the temperature. In recent years the effect of temperature on the interfacial shear strength in polymer matrix composites has been widely studied by a number of investigators by means of the fragmentation test[31,37–45], the pull-out test[46] and the microbond test[47]. In general, the interfacial shear strength decreases as the test temperature increases with a major role being attributed to matrix and interphase thermomechanical properties.

As reported in *Figure 3*, the thermomechanical properties of the nylon-6 matrix used in this work were investigated by the dynamic mechanical thermal analysis. It can be observed that in the range 20– 100°C the elastic modulus strongly decreases from 2000 MPa to 500 MPa, respectively, while the loss factor (tanδ) shows a maximum for a temperature of about 47°C. In *Figure 4* the stress–strain curves of the nylon-6 matrix tested at 20°C and 100°C are reported. The region between the dotted lines represents the strain range where the first fiber break was observed in the microcomposite specimens. It is worth noting that a slight deviation from linearity occurred, thus indicating that the linear elastic hypothesis can be accepted only as a first approximation. An elasto-plastic behavior is apparent and may have a significant effect upon the calculated energy values especially at the higher strains-to-break. The tensile yield stress, determined as the stress where the two tangents to the initial and final parts of the stress–strain curve intersect [48], were found to be 46 MPa at 20°C and 36 MPa at 100°C.

The elastic strain energy, U, obtained by the FE simulation as a function of the debonding length, a, for fibers with different diameters and tested at different temperatures, are reported in *Figure 5*. A strain energy release rate, G, associated to fiber/matrix debonding was then computed from the following relationship:

$$G = -\frac{\partial U}{\partial A} = -\frac{\partial U}{\partial a}\frac{\partial a}{\partial A} \tag{5}$$

where $A = 2\pi r_f$, a is the crack area. The derivative of the

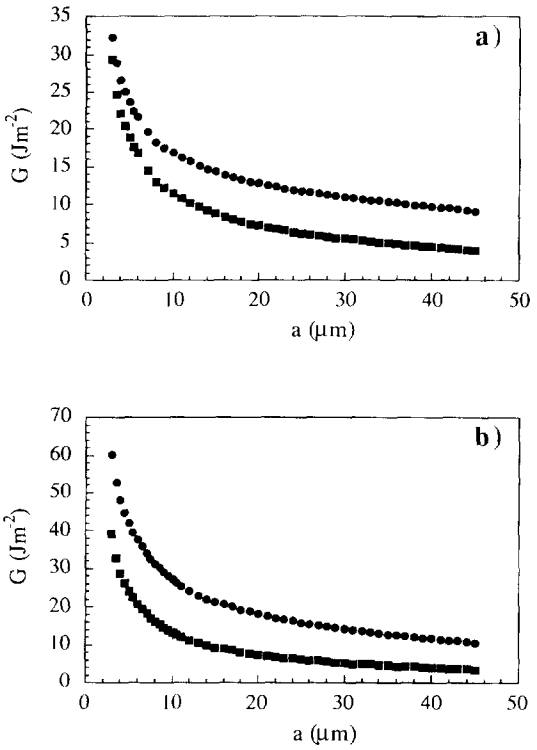

Figure 6 Strain energy release rate, G, as a function of the crack length, a, for (a) Sisecam diameter 14 μm and (b) PPG 2001 diameter 24 μm E-glass fibers at (●) 20°C and (■) 100°C

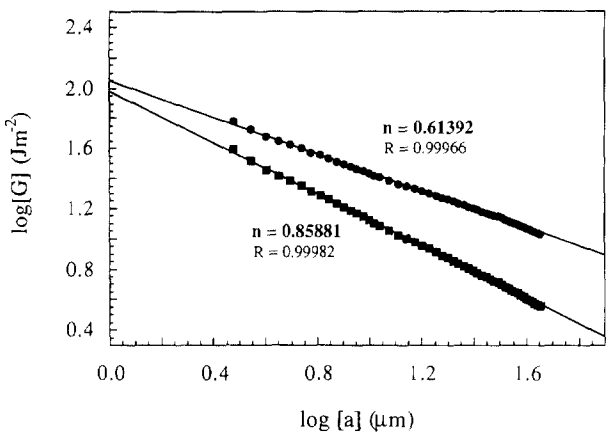

Figure 7 Logarithm of the strain energy release rate, log[G], as a function of the logarithm of the crack length, log[a], for the PPG 2001E-glass fibers at (●) 20°C and (■) 100°C

energy curve was then evaluated by a numerical procedure in order to obtain $\partial U/\partial a$ values to introduce into equation (5). Although the technique based on the representation of all data by a single fitting function is often satisfactory for integration, it usually leads to results as erroneous as those from the simple difference technique. A numerical procedure based on the 'movable strip' technique[49] was therefore preferred. According to this method, the best estimate of the derivative at a point is to fit a function to several data points on both sides of the particular point and then differentiate the resulting function analytically at that point. A smoothing procedure of the experimental data is suggested before the differentiation is performed. In our case a smoothing procedure was repeated four times, a third order polynomial was chosen as fitting function, and seven points were considered for each strip.

The curves of the strain energy release rate as a function of the debonding length are reported in *Figure 6* for a strain of 1%. The G values at very short crack lengths (i.e. a less than 2.5 μm) and very long crack lengths (i.e. a greater than 45 μm) are not reported because they are probably affected by errors related to both the 'edge effects' of the FE model and the 'movable strip' technique adopted for the numerical derivation of the energy curves. As a consequence of the 'fixed grip' boundary conditions adopted in our FE model, the strain energy release rate curves decreased as the crack length increased. For a fixed crack length, the higher the temperature, the lower the G values, i.e. a lower energy was found to be released as the crack propagated at the fiber/matrix interface. For a linear elastic body in the case of 'fixed grips' loading, it is well known that the analytical expression of the strain energy release rate is the following [50]:

$$G = \frac{U_i}{BC}\left(\frac{\partial C}{\partial a}\right) \tag{6}$$

where U_i is the elastic strain energy initially stored in the system, B and C are the sample thickness and compliance, respectively. In the case of the Double Cantilever Beam (DCB) specimen for Mode I fracture testing, the system compliance may be obtained from the elastic beam theory as:

$$C = \frac{2a^3}{3EI} \tag{7}$$

where EI is the flexural rigidity of each beam of the specimen[51].

Equations (6) and (7) give:

$$G_I = \frac{3U_i}{Ba} \tag{8}$$

In the case of fiber-matrix debonding, the opening mode should be described in terms of a combined Mode I and II[16], and the system compliance is an unknown function of the crack length. Nevertheless, the strain energy release rate curves obtained from the FE analysis could be adequately fitted by a power law function in the form:

$$G = \frac{\lambda}{a^n} \tag{9}$$

or

$$\log[G] = \log[\lambda] - n \log a \tag{10}$$

where λ and n are parameters depending on the dimensions of the model (fiber and matrix cylinder radii and lengths), on the materials elastic properties, and the initial strain energy in the system. By way of example, the plot of log[G] as a function of log[a] is reported in *Figure 7* for the PPG 2001 E-glass fiber reinforced system. Parameter n was evaluated through a least square linear regression. As the temperature

increases (i.e. the matrix softened) n was found to increase. Moreover, preliminary results indicate a linear relationship between the parameter n and the fiber radius (*Figure 8*). At present, work is in progress in order to better establish the effect of materials properties and model dimensions on the parameters of equation (9)[52].

Because the analysis is linear-elastic, the G values evaluated at a strain of 1% (*Figure 6*) can be scaled to any other strain ϵ in percent by using the following relationship[13]:

$$G_\epsilon = (\epsilon)^2 G \qquad (11)$$

where G_ϵ is the strain energy release rate corresponding to a strain ϵ.

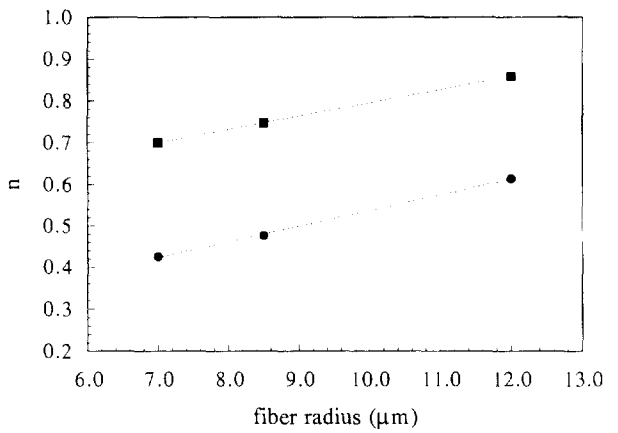

Figure 8 n parameter of equation (9) as a function of the fiber radius at (●) 20°C and (■) 100°C

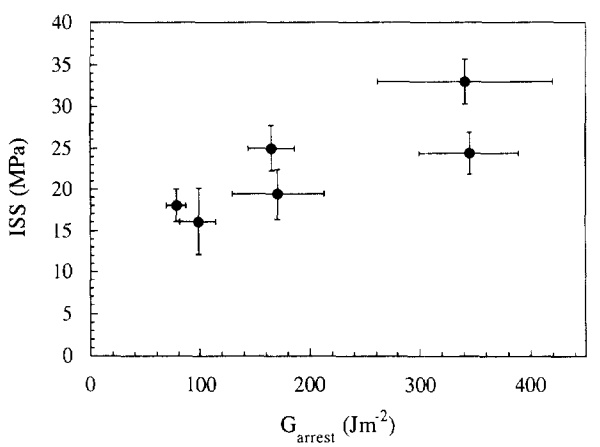

Figure 9 Interfacial shear strength (ISS) versus G_{arrest} for all the samples tested in the present study

In other words, our experiment examines what occurs upon fiber fracture at a given constant strain, i.e. a debond initiates and at constant strain arrests after it attains a specific length. Our fundamental assumption is that the energy dissipated is the critical strain energy release rate for the process, G_{arrest}. If this is truly a material property characterizing the resistance to crack propagation ($G_{arrest} = R$), one can use it to predict the debond length as a function of the stress at which the fiber broke. Consequently, the parameter G_{arrest} could be viewed as a measurement of the dynamic fracture toughness of the fiber-matrix interface.

The resulting G_{arrest} values for the various fiber and temperature combinations are reported in *Table 4*. At room temperature, the unsized E-glass fibers showed a mean G_{arrest} value of 165 Jm^{-2}, while the surface coated fibers were characterized by higher G_{arrest} values of 341 Jm^{-2} for the polyamide compatible and 345 Jm^{-2} for the epoxy compatible sized, respectively. Experimental data obtained at a temperature of 100°C indicated lower G_{arrest} values of 78 Jm^{-2} for the unsized E-glass fibers up to 171 Jm^{-2} and 98 Jm^{-2} for the polyamide and epoxy compatible sized fibers, respectively.

In *Table 4* the interfacial shear strength (ISS) values for the various systems are also reported. As evidenced in *Figure 9*, where ISS is reported versus G_{arrest}, a relationship between the shear strength and fracture toughness of the interface seems to exist. In particular, the higher the fiber/matrix debonding energy the higher the shear strength of the interface.

The interface properties (G_{arrest} and ISS) decrease as the test temperature increases. As previously reported[32,53–55], the decrease of the interfacial shear strength could be explained by a decrease in elastic modulus and shear strength of the matrix with increasing temperature. In particular the transfer of shear stress between the matrix and the fiber is strongly related to the ratio of fiber to matrix modulus. In particular, the shear lag model proposed by Cox[56] predicts that, to a first approximation, the fiber critical length varies as the square root of this ratio. Nevertheless, Cox's analysis neglects the local stress concentration effects near fiber ends. Using a finite difference technique, Termonia[57] showed that, at constant fiber diameter the critical length is linearly related to the ratio of fiber to matrix modulus.

CONCLUSIONS

In this work an experimental method, recently proposed

Table 4 Strain energy release rate at crack arrest, G_{arrest} and interfacial shear strength, ISS, as measured at different temperatures for various nylon-6/E-glass fiber microcomposites

Fiber	Sizing	Test temperature (°C)	Strain energy release rate G_{arrest} (Jm^{-2})	Interfacial shear strength ISS (MPa)
Sisecam	none	20	165 ± 21	25.0 ± 2.8
		100	78 ± 9	18.0 ± 2.0
Sisecam	polyamide compatible	20	341 ± 79	33.0 ± 2.7
		100	171 ± 42	19.4 ± 3.0
PPG 2001	epoxy compatible	20	345 ± 45	24.4 ± 2.5
		100	98 ± 16	16.1 ± 4.0

by the authors for the evaluation of an interfacial fracture toughness parameter, has been applied to nylon-6 matrix E-glass single fiber composites with different sizings. A linear elastic finite element analysis was used in combination with the experimental data in order to evaluate the strain energy release rate associated with the arrest of an interfacial crack, G_{arrest}. The effect of the temperature on the interfacial toughness was also investigated. The experimental value of G_{arrest} obtained at room temperature was equal to 165 Jm^{-2} for the unsized E-glass fibers and to about 342–345 Jm^{-2} for the polyamide and epoxy compatible E-glass sized fibers, respectively. Tests performed at 100°C resulted in a strong reduction of the G_{arrest} values to 78 Jm^{-2} for the unsized fibers and to 171–98 Jm^{-2} for the polyamide and epoxy compatible sized fibers, respectively. A similar temperature dependence was found for the interfacial shear strength, evaluated by the traditional Kelly–Tyson approach.

ACKNOWLEDGEMENTS

This work was partially supported by C.N.R. Comitato Tecnologico, Rome, Italy. Sisecam A.S. (Turkey), and PPG Industries Fiber Glass bv (The Netherlands) are kindly acknowledged for the provision of the glass fibers. The authors wish to thank Dr M. R. Gurvich for helpful discussion of many aspects of this work.

REFERENCES

1. Herrera-Franco, P.J. and Drzal, L.T., Comparison of methods for the measurements of fibre/matrix adhesion in composites. *Composites*, 1992, **23**, 2–27.
2. Narkis, M. and Chen, J.H., Review of methods for characterization of interfacial fibre-matrix interactions. *Polymer Composites*, 1988, **9**, 245–251.
3. Kelly, A. and Tyson, W.R., Tensile properties of fiber-reinforced metals/copper/tungsten and copper/molybdenum. *J. Mech. Phys. Solids*, 1965, **13**, 329–350.
4. Fraser, A.A., Ancker, F.H. and DiBenedetto, A.T., A computer modelled single filament technique for measuring coupling and sizing agent effects in fibre reinforced composites. In *Proceedings of the 30th Annual Tech. Conf. on Reinf. Plastics*, The Society of the Plastics Industry Inc., Washington D.C. USA, 1975, paper 22-A, pp. 1–13.
5. Broutman, L.J., Measurement of the fiber-polymer matrix interfacial strength. In *Interfaces in Composites*, ASTM STP 452, American Society for Testing and Materials, 1969, pp. 27–41.
6. Miller, B., Muri, P. and Rebenfeld, L., A microbond method for determination of the shear strength of a fiber/resin interface. *Comp. Sci. and Techn.*, 1987, **28**, 17–32.
7. Mandell, J.F., Chen, J.H. and McGarry, F.J., A microdebonding test for in-situ fiber-matrix bond and moisture effects. Res. Rep. R80-1. Department of Materials Science and Engineering, Massachusetts Institute of Technology, Feb. 1980.
8. Kim, J.K., Zhou, L. and Mai, Y.W., Stress transfer in the fibre fragmentation test. Part 1. An improved analysis based on a shear strength criterion. *Journal of Material Sciences*, 1993, **28**, 6233–6245.
9. Feillard, P., Désarmot, G. and Favre, J.P., Theoretical aspects of the fragmentation test. *Comp. Sci. and Techn.*, 1994, **50**, 265–279.
10. Asloun, El.M., Donnet, J.B., Guilpan, G., Nardin, M. and Schultz, J., On the estimation of the tensile strength of carbon fibres at short lengths. *Journal of Material Sciences*, 1989, **24**, 3504–3510.
11. Dai, S.-R. and Piggot, M.R., The strengths of carbon and Kevlar fibres as a function of their lengths. *Comp. Sci. and Techn.*, 1993, **49**, 81–87.
12. DiBenedetto, A.T., Measurement of the thermomechanical stability of interphases by the embedded single fiber test. *Comp. Sci. and Techn.*, 1991, **42**, 103–123.
13. DiAnselmo, A., Accorsi, M.L. and DiBenedetto, A.T., The effect of an interphase on the stress and energy distribution in the embedded single fibre test. *Comp. Sci. and Techn.*, 1992, **44**, 215–225.
14. DiBenedetto, A.T., Connelly, S.M., Lee, W.C. and Accorsi, M.L., The properties of organosiloxane/polyester interfaces at an E-glass fiber surface. *J.Adhesion*, 1995, **52**, 41–64.
15. Jones, K.D. and DiBenedetto, A.T., Experimental evaluation of finite element analysis of fracture in the interphase between a fiber and a thermosetting matrix. In *Proceedings of the 3rd International Conference on Deformation and Fracture of Composites*, Guildford, UK, March 1995, pp. 86–95.
16. Pegoretti, A., Accorsi, M.L. and DiBenedetto, A.T., Fracture toughness of fiber-matrix interface in glass-epoxy composites. *Journal of Material Sciences*, 1996, **31**, 6145–6153.
17. Wagner, H.D. and Ling, S., An energy-based interpretation of interfacial adhesion from single fibre composite fragmentation testing. *Advanced Composites Letters*, 1993, **2**(5), 169–172.
18. Wagner, H.D. and Lustinger, A., Effect of water on the mechanical adhesion of the glass/epoxy interface. *Composites*, 1994, **24**(7), 613–616.
19. Wagner, H.D., Nairn, J.A. and Detassis, M., Toughness of interfaces from initial fiber-matrix debonding in a single. *Appl. Comp. Mat.*, 1995, **2**, 107–117.
20. Detassis, M., Frydman, E., Vrieling, D., Zhou, X.-F., Wagner, H.D. and Nairn, J.A., Interface toughness in fibre composites by the fragmentation test. *Composites Part A*, 1996, **27**, 769–773.
21. Copponex, T.J., Analysis and evaluation of the single fibre fragmentation test. *Comp. Sci. and Techn.*, 1996, **56**, 893–909.
22. Nairn, J.A., A variational mechanics analysis of the stresses around breaks in embedded fibers. *Mech. Mater.*, 1992, **13**, 131–157.
23. Chua, P.S. and Piggot, M.R., The glass fibre-polymer interface: II—Work of fracture and shear stresses. *Comp. Sci. and Techn.*, 1985, **22**, 107–1192.
24. Piggot, M.R., Debonding and friction at fiber–polymer interfaces. I: criteria for failure and sliding. *Comp. Sci. and Techn.*, 1987, **30**, 295–306.
25. Penn, L.S. and Lee, S.M., Interpretation of experimental results in the single pull-out filament test. *J.Comp.Techn. and Res.*, 1989, **11**, 23–30.
26. Zhou, L., Kim, J.K. and Mai, Y.W., Interfacial debonding and fibre pull-out stresses. Part II. A new model based on the fracture mechanics approach. *Journal of Material Sciences*, 1992, **27**, 3155–3166.
27. Jiang, K.R. and Penn, L.S., Improved analysis and experimental evaluation of the single filament pull-out test. *Comp. Sci. and Techn.*, 1992, **45**, 89–103.
28. Hampe, A. and Marotzke, C., The fracture toughness of glass fibre-polymer matrix interface: measurement and theoretical analysis. In *Proceedings of the 3rd International Conference on Deformation and Fracture of Composites*, Guildford, UK, March 1995, pp. 86–95.
29. Scheer, R.J. and Nairn, J.A., A comparison of several fracture mechanics methods for measuring interfacial toughness with microbond tests. *J.Adhesion*, 1995, **53**, 45–64.
30. Gurvich, M.R., DiBenedetto, A.T. and Pegoretti, A., On evaluation of the statistical parameters of a Weibull distribution. *J.Mat.Sci.*, 1997, **32**, 3711–3716.
31. Detassis, M., Pegoretti, A. and Migliaresi, C., Effect of temperature and strain rate on interfacial shear stress transfer in carbon/epoxy model composites. *Comp. Sci. and Techn.*, 1995, **53**, 39–46.
32. Ohsawa, T., Nakayama, A., Miwa, M. and Hasegawa, A., Temperature dependence of critical fiber length for glass fiber-reinforced thermosetting resins. *J. Appl. Pol. Sci.*, 1978, **22**, 3203–3212.
33. Hollaway, L., *Handbook of Polymer Composites for Engineers*, Woodhead Publishing, Cambridge, UK, 1994, p. 28.
34. Brandrup, J. and Immergut, E.H., *Polymer Handbook*, John Wiley, New York, 1989, pp. V–115.
35. Mullin, J., Berry, J.M. and Gatti, A., Some fundamental fracture mechanisms applicable to advanced filament reinforced composites. *J. Comp. Mater.*, 1968, **2**, 82–103.
36. Feillard, P., Désarmot, G. and Favre, J.P., A critical assessment of the fragmentation test for glass/epoxy systems. *Comp. Sci. and Techn.*, 1993, **49**, 109–119.

37. Detassis, M., Pegoretti, A., Migliaresi, C. and Wagner, H.D., Experimental evaluation of residual stresses in single fiber composites by means of the fragmentation test. *Journal of Material Sciences*, 1996, **31**, 2385–2392.
38. Asloun, El.M., Nardin, M. and Schultz, J., Stress transfer in single-fibre composites: effect of adhesion, elastic modulus of fibre and matrix, and polymer chain mobility. *Journal of Material Sciences*, 1989, **24**, 1835–1844.
39. DiBenedetto, A.T. and Lex, P.J., Evaluation of surface treatments for glass fibers in composite materials. *Pol. Eng. and Sci.*, 1989, **29**, 543–555.
40. Fraser, W.A., Ancker, F.H., DiBenedetto, A.T. and Elbirli, B., Evaluation of surface treatments for fibers in composite materials. *Polym. Comp.*, 1983, **4**, 238–248.
41. Wimolkiatisak, A.S. and Bell, J.P., Interfacial shear strength and failure modes of interphase-modified graphite-epoxy composites. *Polym. Comp.*, 1989, **10**, 162–172.
42. Rao, V. and Drzal, L.T., The temperature dependence of interfacial shear strength for various polymeric matrices reinforced with carbon fibers. *J.Adhesion*, 1992, **37**, 83–95.
43. Skourlis, T.P. and McCullough, R.L., The effect of temperature on the behaviour of the interphase in polymeric composites. *Comp. Sci. and Techn.*, 1993, **49**, 363–368.
44. Pegoretti, A., Della Volpe, C., Detassis, M., Migliaresi, C. and Wagner, H.D., Thermomechanical behaviour of interfacial region in carbon fibre/epoxy composites. *Composites Part A*, 1996, **27**, 1067–1074.
45. DiLandro, L. and Pegoraro, M., Evaluation of residual stresses and adhesion in polymer composites. *Composites Part A*, 1996, **27A**, 847–853.
46. Auvray, M.H., Chéneau-Henry, P., Leroy, F.H. and Favre, J.P., Pull-out testing of carbon/bismaleimide systems in the temperature range 20–250°C. *Composites*, 1994, **25**, 776–780.
47. Straub, A., Slivka, M. and Schwartz, P., Time and temperature effects on the interface strength using the microbond test. *Comp. Sci. and Techn.* in press.
48. Ward, I.M., *Mechanical Properties of Solid Polymers*, John Wiley, 2nd edn. Chichester, 1985, p. 337.
49. Hershey, H.C., Zakin, J.L. and Simha, R., Numerical differentiation of equally spaced and not equally spaced experimental data. *Ind. Eng. Chem.*, 1967, **6**, 413–421.
50. Matthews, F.L. and Rawlings, R.D., *Composite Materials: Engineering and Science*, Chapman and Hall, London, UK, 1994, p. 327.
51. Carlsson, L.A. and Pipes, R.B., *Experimental Characterization of Advanced Composite Materials*, Prentice-Hall, New Jersey, USA, 1987, p. 160.
52. Pegoretti, A., Fidanza, M. and Migliaresi, C., manuscript in preparation.
53. Asloun, El. M., Nardin, M. and Schultz, J., Stress transfer in single-fibre composites: effect of adhesion, elastic modulus of fibre and matrix, and polymer chain mobility. *Journal of Material Science*, 1989, **24**, 1835–1844.
54. Ogata, N., Yasumoto, H., Yamasaki, K., Yu, H., Ogihara, T., Yanagawa, T., Yoshida, K. and Yamada, Y., Evaluation of interfacial properties between carbon fibres and semycrystalline thermoplastic matrices in single-fibre composites. *Journal of Material Sciences*, 1992, **27**, 5108–5112.
55. Monette, L., Anderson, M.P., Ling, S. and Grest, G.S., Effect of modulus and cohesive energy on critical fibre length in fibre-reinforced composites. *Journal of Material Sciences*, 1992, **27**, 4393–4405.
56. Cox, H.L., The elasticity and strength of paper and others fibrous materials. *Brit.J.Appl.Phys.*, 1952, **3**, 72–79.
57. Termonia, Y., Theoretical study of the stress transfer in single fibre composites. *Journal of Material Science*, 1987, **22**, 504–508.